

## Excitation spectroscopy of the In-related isoelectronic bound exciton under uniaxial stress and magnetic-field perturbations

S. P. Watkins and M. L. W. Thewalt

*Department of Physics, Simon Fraser University, Burnaby, British Columbia, Canada V5A 1S6*

(Received 24 February 1986)

The photoluminescence excitation spectrum of the In-related isoelectronic bound exciton in Si is studied by means of a tunable optical parametric oscillator in conjunction with uniaxial stress and magnetic field perturbations. The hole is shown to be highly localized on a defect with a  $C_{2v}$ -symmetry strain field which completely quenches the hole orbital angular momentum. The exciton ground state is split by the unusually large value of 11.4 meV by the exchange interaction into a spin triplet at 1118 meV and a spin singlet at 1129.4 meV. Such a large splitting indicates a much more localized electron state than one would expect for an effective-mass-like state. It is proposed that a higher-lying state at 1154.3 meV is due to a  $\Gamma_3(T_d)$  valley-orbit excited state of the electron.

### I. INTRODUCTION

The physical process whereby an electrically neutral defect in a semiconductor, for example  $N_P$  in GaP, can bind an electron-hole pair, or exciton, has motivated a great deal of study in past years. The simplest model, due to Hopfield, Thomas, and Lynch<sup>1</sup> (HTL) assumes that such defects introduce a short-range potential which binds one of the particles in a localized state with the other bound in turn by the Coulombic potential introduced by the first particle. Cohen and Sturge<sup>2</sup> confirmed this model in a convincing fashion for the case of the near-neighbor nitrogen-nitrogen pairs substituting for P in GaP, by means of photoluminescence excitation (PLE) spectroscopy, using a tunable dye laser to scan the absorption spectrum of the acceptorlike excited states of the hole, which was shown to be bound in the Coulombic potential of a very tightly localized electron. In the notation of Cohen and Sturge, the  $i$ th nearest-neighbor pair is denoted  $NN_i$ . For some of the more distant pairs, e.g., for  $i > 7$ , and for the case of isolated  $N$ , there is some question as to whether the electron has a bound state in the absence of the hole.

Some years ago Allen<sup>3</sup> proposed an alternate model of isoelectronic binding in which the local strain well caused by an isoelectronic defect generates a potential which is more slowly varying, but attractive to both electrons and holes. Recently Monemar *et al.*<sup>4</sup> and Gislason *et al.*<sup>5</sup> have applied PLE to the study of two Cu-related isoelectronic defects in GaP for which the electron and hole appear to be bound by a deep potential which is attractive to both particles. The excited-state spectrum revealed a very large splitting due to the exchange interaction between the bound hole and electron, and no evidence of a series of hydrogenic excited states of either particle. In both cases a strong defect-induced strain field was invoked to account for the unusual degree of localization of both particles.

Recently a variety of photoluminescence (PL) emission lines in Si have been identified as originating from the recombination of excitons bound to electrically neutral ag-

gregates of impurities, i.e., isoelectronic bound excitons (IBE's). Wagner and Sauer<sup>6</sup> used a tunable color center laser to probe the acceptorlike excited-state spectrum of the  $N$ -related isoelectronic bound exciton spectrum at 1122.3 meV. The PLE spectrum of excitons bound to neutral Be-Be pairs was recently obtained by Thewalt *et al.*<sup>7</sup> using a white light source filtered through a monochromator. This excited-state spectrum was subsequently interpreted by the far-infrared studies of Labrie *et al.*<sup>8</sup> in which the states were shown to correspond to those of a hole bound in a Coulombic potential. Recently Thonke *et al.*<sup>9</sup> have interpreted PLE transitions observed from the 790 meV defect in electron-irradiated Si as being due to effective mass donorlike excited states of an isoelectronic bound exciton. A similar model was used by Wagner *et al.* to explain the excited-state spectrum of the thermally induced 767 meV defect in oxygen-rich Si.<sup>10</sup> All of the above cases were consistent with the HTL model of IBE's.

The In-related photoluminescence emission at 1118 meV was one of the first of a growing list of emission lines to be identified as due to the recombination of IBE's in Si.<sup>11,12</sup> The 4.2 K PL emission consists of an intense, narrow no-phonon line at 1118 meV ( $P_0^0$  line) and a strong band of non-momentum-conserving phonon replicas, indicative of a highly localized electronic state. The PL properties have been thoroughly investigated by a variety of techniques including transient excitation, thermal activation, uniaxial stress, and Zeeman measurements.<sup>13,14</sup> Wagner and Sauer have reported the PLE spectrum of the In-related isoelectronic defect in the absence of external perturbations using a color center laser.<sup>15</sup> They reported a set of three strong, widely spaced absorption lines,  $P_0^0$ ,  $P_2^0$ , and  $P_3^0$  with a markedly nonhydrogenic energy spacing. No model has been provided as to the anomalous character of this spectrum.

In this study PLE spectroscopy with a tunable parametric oscillator was used in conjunction with uniaxial stress and magnetic field perturbations to explain the electronic excited-state spectrum seen previously in PLE. First, the symmetry of the defect is identified as rhombic

I ( $C_{2v}$ ) from the stress splittings of the lowest-lying exciton states,  $P_0^0 P_2^0$ . It is shown via selective excitation that the stress splittings of the two lowest-lying states are purely orientational. Zeeman measurements are used to show that the exciton ground state is split by the exchange interaction into a ground-state triplet ( $P_0^0$  line) and a singlet ( $P_2^0$  line) with an unusually large splitting energy of 11.4 meV. This splitting is much larger than previously reported values in Si, which were of the order of 2–3 meV, and indicates considerable electron-hole overlap arising from an electron that is more deeply bound than in the usual HTL case. In this respect, the excited-state spectrum resembles that of the recently reported IBE in GaP:Cu.<sup>4,5</sup> Such behavior is consistent with a “quenching” of the orbital angular momentum of the tightly bound hole in the low-symmetry  $C_{2v}$  defect field which causes it to behave like a pure spin  $\frac{1}{2}$  particle. The polarization dependence of the magnetic field results for the two lowest-lying exciton states is explained by making simple assumptions about the symmetries of the electron and hole wave functions.

An interesting feature revealed by the stress data is the presence of extra degeneracy in the highest-lying exciton transition,  $P_3^0$ . It is proposed that this level is due to an excited state of the electron, which is derived from the  $1s \Gamma_3$  ( $T_d$ ) valley-orbit state. The unperturbed electron states of the two lowest-lying exciton levels are assumed to derive from the  $1s \Gamma_1$  ( $T_d$ ) valley-orbit states. The observed nonlinearity of the  $\langle 001 \rangle$  stress splittings of the lowest-lying exciton levels is thus modeled by a stress-induced mixing of the  $\Gamma_1$  and  $\Gamma_3$   $1s$  electron states assuming a somewhat reduced value of the electron deformation potential,  $\Xi_u$ . The large value of the  $1s \Gamma_1$ -to- $\Gamma_3$  splitting is also consistent with our conclusion that the short-range potential of this defect is attractive for electrons as well as for holes.

## II. EXPERIMENTAL

Samples were cut from a boule of commercially grown In-doped, float-zoned Si ( $2 \times 10^{16}$  In atoms/cm<sup>3</sup>). The samples were oriented along the three principal crystallographic directions and cut into rectangular slabs of dimensions  $1 \times 2 \times 8$  mm<sup>3</sup>. The samples were subjected to a rapid quench from 1100°C to room temperature in order to greatly enhance the luminescence intensity.<sup>13</sup>

Stress was applied by means of a vacuum-activated diaphragm and directly measured by means of a calibrated load cell. Zeeman measurements were carried out in a split-pair 10-T superconducting magnet cryostat. All experiments were carried out with the samples immersed in liquid He at 4.2 K.

Luminescence was dispersed by a  $\frac{3}{4}$ -m double grating spectrometer, and detected by a Varian InGaAsP photomultiplier with associated photon counting electronics.<sup>13</sup>

Tunable excitation in the 1100–1170 meV absorption region of these centers was provided by a Chromatix CMX-IR LiNbO<sub>3</sub> optical parametric oscillator (OPO). The pumping source for this device consisted of a narrow linewidth dye laser which was excited by a continuously pumped, Q-switched, frequency-doubled Nd:YAG laser

operating at a 1–2 kHz repetition rate. The pumping arrangement is similar in principle to that of Wallace,<sup>16</sup> with the exception that it employs a much simpler dye-laser cavity employing a short-cavity grazing-incidence-grating arrangement.<sup>17</sup> The typical OPO output power was 20–40 mW with 2 W of average Nd:YAG power at 532 nm and 400 mW of dye-laser output at 610–630 nm. The spectral linewidth of the OPO output was 0.2–0.3 meV.

## III. RESULTS

The zero-field excitation spectrum for the Si:In isoelectronic center is shown by the lower spectrum in Fig. 1. This spectrum is identical to the one first observed by Wagner and Sauer,<sup>15</sup> whose labeling convention we use here. The spectrum represents the emission intensity of the dominant  $P_0^0$  PL transition as a function of excitation energy. Because of the long 200  $\mu$ s linewidth lifetime of these centers at 4.2 K, it was possible to scan the laser energy over the  $P_0^0$  luminescence transition by rejecting scattered laser light during the actual firing of the laser pulse by means of a chopper wheel synchronized to the laser pulse train. In addition to the  $P_0^0$  line, which is the predominant PL transition, two even stronger no-phonon excited states labeled  $P_2^0$  and  $P_3^0$  are observed at energies 11.4 and 36.4 meV above  $P_0^0$ . The  $P_3^0$  transition energy of 1154.3 meV is almost exactly coincident with the free-exciton no-phonon energy of 1154.6 meV, so this state is only bound by a few tenths of an meV. In addition to the three principal no-phonon transitions, a variety of broader anti-Stokes phonon replicas are observed. These have been discussed in detail by Wagner and Sauer.<sup>15</sup> This

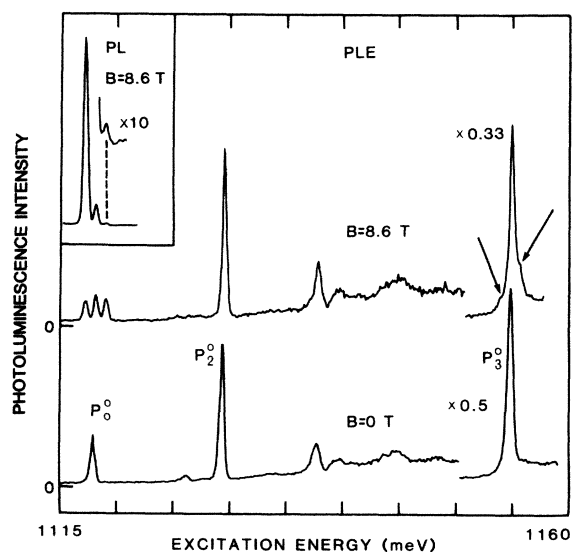


FIG. 1. Excitation spectrum of the In isoelectronic bound exciton with magnetic fields of zero and 8.6 T, monitoring the total PL intensity of the  $\sim 1118$  meV  $P_0^0$  no-phonon lines. Note the weak shoulders on the  $P_3^0$  line upon application of the field. The inset shows the PL spectrum obtained at the observation temperature of 4.2 K showing the strong thermalization of the Zeeman subcomponents of  $P_0^0$ , which is of course not observed in the excitation spectrum.

spectrum is quite different from any of the shallow acceptorlike or donorlike spectra observed in other isoelectronic centers in Si to date, which consisted of a set of absorption lines decreasing in intensity with increasing energy, and converging to an ionization limit of 30–40 meV above the ground-state transition.<sup>6,7,9,10</sup>

The magnetic field dependence of the  $P_0^0$  line has been discussed in a previous work which involved only PL measurements.<sup>14</sup> In that work it was demonstrated that the  $P_0^0$  line splits into a triplet with a splitting that was independent of the direction of the applied field, and this fact was used to argue that the hole orbital angular momentum was quenched by a low symmetry defect field. The upper excitation spectrum in Fig. 1 shows the effect of an 8.6 T magnetic field on the excited states. The  $P_0^0$  line splits with an effective  $g$  value of 2.0, while the  $P_2^0$  line does not split for fields up to 8.6 T. This behavior is consistent with the coupling of two spin  $\frac{1}{2}$  particles to form a spin triplet and a spin singlet with an exchange interaction energy of 11.4 meV. This spectrum was obtained by monitoring the PL intensity at the zero-field  $P_0^0$  energy, with the spectrometer slits opened wide enough to accept all three PL transitions. Identical spectra were obtained by selectively monitoring any of the three magnetically split  $P_0^0$  subcomponents, the only difference being due to the different signal strengths caused by the extreme thermalization of the PL subcomponents (see inset, Fig. 1). This behavior is expected for a purely electronic splitting, and differs from the case of the stress splittings discussed below, which are due solely to orientational effects.

Although  $P_3^0$  at first appeared to remain essentially unsplit in an 8.3 T field, a closer examination revealed evidence of shoulders forming on either side of the zero-field energy, consistent with an effective  $g$  value close to 2.0, but with a rather low intensity (see upper excitation spectrum, Fig. 1). It will be argued below that the nature of the electron state responsible for  $P_3^0$  results in a negligible exchange splitting, leading to a superposition of a strong

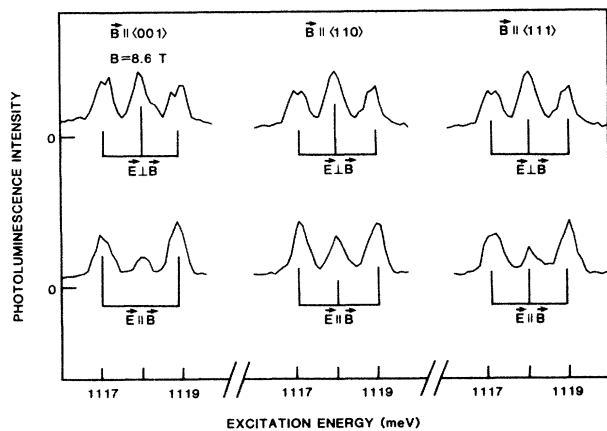


FIG. 2. Excitation spectrum of the  $P_0^0$  line with the electric field of the exciting radiation alternately parallel or perpendicular to the 8.6 T magnetic field. The polarization dependence is the opposite of that expected for a pure spin triplet with full rotational symmetry. The length of the bars under each component is proportional to the relative strength of that component as calculated using the model described in the text.

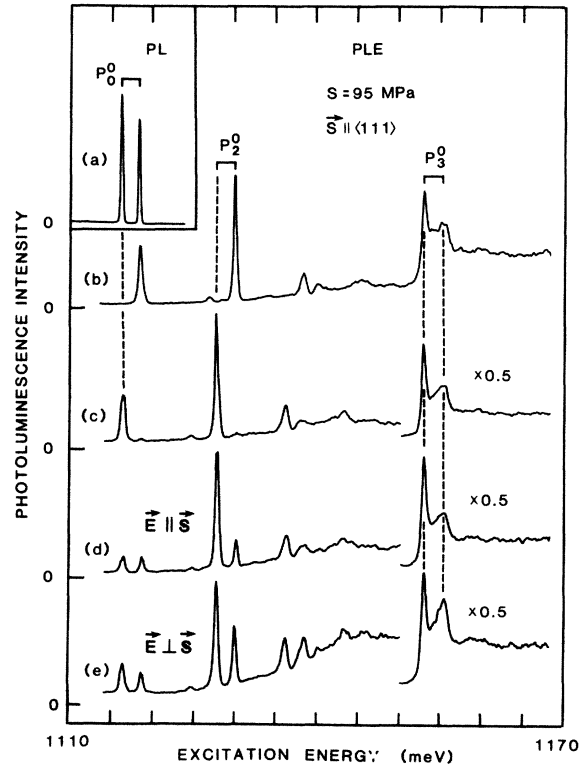


FIG. 3. Inset (a): PL spectrum of the  $P_0^0$  line under a 95 MPa stress along the  $\langle 111 \rangle$  axis showing the lack of thermalization at 4.2 K. (b) and (c): The excitation spectra obtained when monitoring the upper or lower PL subcomponents of  $P_0^0$ , respectively. These spectra confirm that the splittings of  $P_0^0$  and  $P_2^0$  are due solely to orientational degeneracy. (d) and (e): The excitation spectra obtained by polarizing the excitation beam, parallel or perpendicular to the stress axis. In these spectra the spectrometer bandpass was greatly increased in order to collect signal from both  $P_0^0$  PL components simultaneously.

singlet and a weak triplet transition, thus explaining the low intensity of the shoulders.

Figure 2 is a summary of the polarization dependence of the magnetic subcomponents of the  $P_0^0$  triplet transition for the case in which the polarization of the excitation beam is either parallel or perpendicular to the magnetic field. Excitation was in all cases approximately along the  $\langle 110 \rangle$  crystal axis. It is interesting to note that this polarization dependence is the opposite of that expected for electric-dipole transitions from a spin-triplet state to a spin-singlet state in a system with full rotational symmetry. This feature will be explained below.

Figure 3 summarizes the important features of the PLE spectrum under a uniaxial stress of 95 MPa in the  $\langle 111 \rangle$  direction. Inset (a) shows the splitting of the  $P_0^0$  line as observed in PL with above-gap excitation under the same conditions. The stress dependence of this line was previously investigated by means of PL, and on the basis of a lack of thermalization of the subcomponents for stress along any of the three major axes, it was concluded that the splittings were purely orientational.<sup>14</sup> This is confirmed in a convincing fashion by the PLE spectra of Figs. 3(b) and 3(c) in which the PL emission is monitored at the upper and lower stress-split  $P_0^0$  components, respec-

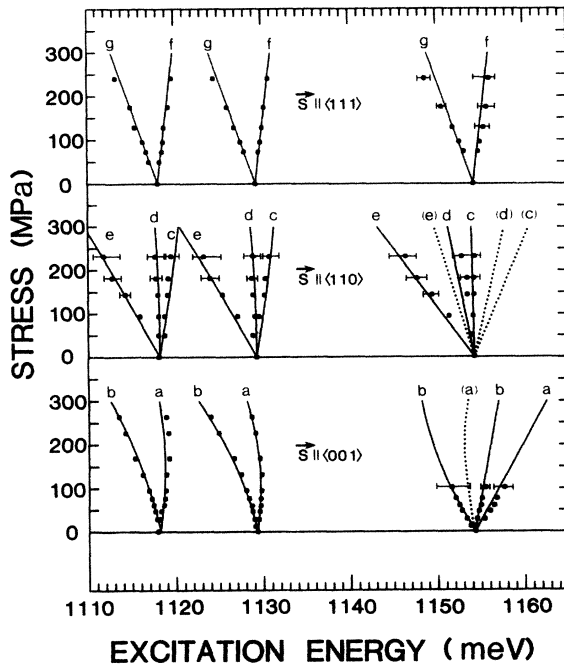


FIG. 4. Summary of the stress splittings of the three principal lines for stresses along the three main crystal axes. For  $\langle 111 \rangle$  stress all three lines split with roughly the same shift rate. For  $\langle 001 \rangle$  stress  $P_0^0$  and  $P_2^0$  split in a similar fashion, although the  $P_2^0$  splitting is more nonlinear. In addition,  $P_3^0$  shows extra degeneracy consistent with a  $\Gamma_3 (T_d)$  electron excited state. Lines represent fits using the simple valley-orbit model described in the text. Dotted lines are predicted lines which are not observed in practice, probably due to the large broadenings due to the resonance or near resonance of  $P_3^0$  components with free-exciton states.

tively. For the case of the  $P_0^0$  and  $P_2^0$  resonances, excitation only occurs into the defect orientation corresponding to the PL energy being monitored. The behavior of  $P_3^0$  is more complicated. Under  $\langle 111 \rangle$  stress  $P_3^0$  splits into two components with the same shift rates as  $P_0^0$  and  $P_2^0$ , but the upper component becomes quite broad. In addition, both components are observed simultaneously while monitoring either of the  $P_0^0$  subcomponents. This is probably due to the fact that  $P_3^0$  is essentially resonant with the free-exciton no-phonon energy, permitting excitation transfer from one class of defect orientations to the other via free-exciton generation and subsequent recapture. It is interesting to note that there is nonetheless a small enhancement of the lower  $P_3^0$  absorption strength when monitoring at the lower  $P_0^0$  PL energy. In Figs. 3(d) and 3(e), the entrance and exit slits of the spectrometer were opened up to the point where the spectral bandpass of the spectrometer exceeded the splitting of the  $P_0^0$  components. In this way both  $P_0^0$  components could be monitored in the same scan and the relative effect of polarization of the excitation beam could be determined.

Figure 4 represents a summary of the stress splittings for all three principal stress directions. The  $P_0^0$  stress splittings agree well with our earlier PL data.<sup>14</sup> As in the case of the PLE data under  $\langle 111 \rangle$  stress, excitation into a given  $P_0^0$  or  $P_2^0$  stress-split component only occurred if the corresponding  $P_0^0$  PL component was monitored, confirm-

ing that these splittings are purely orientational. Unfortunately the  $\langle 110 \rangle$  stress data were somewhat broadened by inhomogeneous stress, which is reflected in the broad linewidths indicated by the error bars, but comparisons with the previous PL data do not indicate a large discrepancy in the energy splittings. For the other stress directions, the stress homogeneity was very good and yielded  $P_0^0$  PL linewidths of no greater than 0.4 meV right up to the maximum applied stress.

The similarities of the splitting patterns for the  $P_0^0$  and  $P_2^0$  lines are consistent with our proposal that these two lines originate from the recombination of excitons with the same electron and hole states, but with symmetric and antisymmetric total spin functions, respectively.

We have shown that the  $\langle 111 \rangle$  stress splittings of the  $P_3^0$  line are essentially the same as those of the two lower energy lines. Under  $\langle 001 \rangle$  stress however the  $P_3^0$  transition splits into three readily observable components: a sharp central peak whose absorption strength is enhanced when monitoring the lower  $P_0^0$  PL transition, and two broader lines to higher and lower energies. Given the similarity in splitting rate of the upper two  $P_3^0$  components to the  $P_0^0$  and  $P_2^0$  rates it is likely that these two  $P_3^0$  components correspond to the lifting of the same orientational degeneracy but with an additional upward shift of their center of gravity, and that the extra line represents a splitting due to an additional electronic degeneracy of the bound electron. At stresses above 100 MPa the  $P_3^0$  line is soon lost in the rapidly shifting free-exciton edge.

The  $\langle 110 \rangle$  splittings of  $P_3^0$  were rather obscured by the broadening of these lines due to stress inhomogeneities. Nevertheless three principal components were observed, and their shift rates correlate fairly well with those of  $P_0^0$  and  $P_2^0$ , except for a center-of-gravity shift to lower energy. In addition there is some weak structure to higher energy that again indicates extra electronic degeneracy.

#### A. Defect symmetry

The stress splittings of Fig. 4 are consistent with the removal of orientational degeneracy of a rhombic I defect imbedded in a cubic lattice. The point group of such a defect is  $C_{2v}$ , consisting of a twofold axis labeled  $Z$  along a  $\langle 001 \rangle$  or equivalent axis and two reflection planes whose normals, labeled  $X$  and  $Y$ , are perpendicular to that axis and lie along the  $\langle 110 \rangle$  and  $\langle \bar{1}\bar{1}0 \rangle$  or equivalent axes. Such a defect has six equivalent orientations in an unstrained crystal. Under external stress some of these orientations become inequivalent. For  $\langle 111 \rangle$ ,  $\langle 110 \rangle$ , and  $\langle 001 \rangle$  stresses there are, respectively, two, three, and two inequivalent classes, in agreement with the number of components observed for the  $P_0^0$  and  $P_2^0$  transitions. Kaplyanski<sup>18</sup> has derived phenomenological shift expressions which parametrize the shift rates of optical transitions between nondegenerate levels of centers with orientational degeneracy, based solely on symmetry arguments and the assumption that the perturbing potential is a linear function of the stress tensor. For a rhombic I center all seven shift rates can be shown to depend linearly on only three parameters,  $A_1$ ,  $A_2$ , and  $A_3$ . These expres-

sions are given in Table I together with the  $P_0^0$  components to which they correspond. Also listed are the number of equivalent orientations within each subcomponent. These should be reflected in the relative intensities of the PL subcomponents of the  $P_0^0$  line. This is observed to be the case for low stresses although some stress-induced reorientation to the lower energy configurations appears to occur at higher stresses.<sup>14</sup> The experimental shift rates listed in Table I represent the linear component of the least-squared fits to the data in Fig. 4. The method by which these fits were obtained will be described below. The  $A_i$  values quoted in the table are those which best reproduce the observed shifts. The relatively close agreement confirms the correctness of the  $C_{2v}$  designation. It is interesting to note that these shift rates are very close to those obtained by Clifton *et al.*<sup>19</sup> for the case of the 875 meV Ga-related PL transition in electron-irradiated Si, for which  $C_{2v}$  symmetry was also deduced.

### B. Lowest-lying exciton states

The Zeeman data show that the hole behaves essentially like a spin  $\frac{1}{2}$  particle in its coupling to the electron states. This implies that the orbital angular momentum of the hole is "quenched"<sup>20</sup> by the low-symmetry defect field of the impurity. In a perfect cubic crystal, the topmost valence band is threefold degenerate (neglecting spin), and derived from  $l=1$   $p$  states. While it is likely that the exciton binding potential for this particular defect contains strong short-range hole-attractive components, we assume that the basic character of the hole states is still  $p$ -like, with a relatively small admixture of states from higher-lying bands. Similar simplifying assumptions have been used to model other axial IBE's in GaP (Ref. 21) and Si (Ref. 22). A defect-induced strain field, with local coordinate axes  $X$ ,  $Y$ , and  $Z$  can remove some of this  $p$ -state degeneracy, leading to a lowering of one of the  $p_X$ ,  $p_Y$ , or  $p_Z$  states relative to the others. If this lowering of one of the  $p$  states is large compared to the spin-orbit coupling interaction, which tends to mix the stress-split hole states, then the hole state of lowest energy is simply the direct product of a single  $p$  state with the hole spin function. The linear Zeeman Hamiltonian is of the form

$$H_{LZ} = \mu_B \mathbf{B} \cdot (\gamma \mathbf{L} + 2\mathbf{S}),$$

TABLE I. This table shows the shift rates predicted on simple symmetry grounds for a rhombic I ( $C_{2v}$ ) center in a cubic crystal. The letters "a" to "f" label each of the stress components in Fig. 4. The best fit to the seven experimentally observed shift rates was obtained with  $A_1 = 7.0$  meV/MPa,  $A_2 = -11.3$  meV/MPa, and  $A_3 = -17.8$  meV/MPa.

Stress	Component	Energy	Shift Rate (meV/MPa)	
			Measured	Calculated
$\langle 001 \rangle$	$a(2)$	$A_1$	7.5	7.0
	$b(4)$	$A_2$	-10.4	-11.3
$\langle 110 \rangle$	$c(1)$	$A_2 - A_3$	9.0	6.4
	$d(4)$	$(A_1 + A_2)/2$	0.0	-2.2
	$e(1)$	$A_2 + A_3$	-27.0	-29.1
$\langle 111 \rangle$	$e(3)$	$(A_1 + 2A_2 - 2A_3)/3$	5.9	6.6
	$f(3)$	$(A_1 + 2A_2 + 2A_3)/3$	-17.8	-17.1

where  $\mu_B$  and  $\gamma$  are constants and  $\mathbf{L}$  and  $\mathbf{S}$  are the total orbital and spin angular momenta. It is easy to verify that the expectation value of the  $\mathbf{B} \cdot \mathbf{L}$  term in this Hamiltonian with the above single  $p$  state must be zero, leading to a pure spin  $\frac{1}{2}$  behavior. It is often stated that a compressional sign of the local strain field is required to produce such a hole state at lowest energy, but this is true only for strain fields with relatively high symmetry, e.g.,  $C_{3v}$  or  $D_{2h}$ . A  $C_{2v}$  strain field of sufficient strength will always produce such a hole state at lowest energy regardless of the sign of the field, guaranteeing that the hole orbital angular momentum will be quenched (assuming that the spin-orbit coupling constant is relatively small).

The particular  $p$  state which lies lowest in hole energy is determined by the relative magnitudes of the shear components of the  $C_{2v}$  biaxial crystal field. In order to reproduce the polarization results of Figs. 2 and 4, we have assumed that the hole state is derived from either the  $p_X$  or  $p_Y$  hole states, i.e., not from the hole state which is associated with the twofold  $Z$  axis of the defect. Specifically, we assume that the hole state is  $p_X$ , which transforms as the group representation  $\Gamma_2$  in  $C_{2v}$ , while the electron is assumed to transform as the  $\Gamma_1$  ( $C_{2v}$ ) state derived from the lowest valley-orbit electron state. The spin of both particles transforms as the  $\Gamma_5$  ( $C_{2v}$ ) double group. Coupling of the two spin functions together with the electron and hole  $\Gamma_1$  and  $\Gamma_2$  orbital wave functions according to the prescription of Koster *et al.*<sup>23</sup> leads to the following exciton product states which transform as the four one-dimensional (1D) representations of  $C_{2v}$  namely:

$$\Gamma_2: \Psi_2 = p_X(\uparrow\downarrow - \downarrow\uparrow) (P_2^0), \quad (1a)$$

$$\Gamma_1: \Psi_1 = p_X(\uparrow\uparrow + \downarrow\downarrow) (P_0^0),$$

$$\Gamma_3: \Psi_3 = p_X(\uparrow\uparrow - \downarrow\downarrow) (P_0^0), \quad (1b)$$

$$\Gamma_4: \Psi_4 = p_X(\uparrow\downarrow + \downarrow\uparrow) (P_0^0),$$

The dominant term in the exchange interaction of the form:

$$E_{ex} = \Delta \mathbf{S}_h \cdot \mathbf{S}_e,$$

where  $\mathbf{S}_h$  and  $\mathbf{S}_e$  are the hole and electron spin operators

and  $\Delta$  is a constant. This leads to a splitting of the exciton ground state into a  $\Gamma_2$  antisymmetric singlet and the remaining three symmetric basis functions which are partners of a nearly degenerate spin triplet; the orthorhombic splitting which is in principle possible is so small as to be unobservable by optical measurements alone. In principle these splittings could be resolved by optically detected magnetic resonance, as was done for the closely related 1911 meV center in GaP.<sup>5</sup>  $\Delta$  is given by the  $P_2^0$ -to- $P_0^0$  singlet-to-triplet splitting of 11.4 meV.

In the absence of external fields, transitions from the  $\Gamma_2$  singlet to the  $\Gamma_1$  crystal ground state are dipole allowed for radiation with the electric vector parallel to the  $X$  axis. Transitions from the  $\Gamma_1$  and  $\Gamma_4$  level of the triplet are allowed for radiation with the electric vector parallel to the  $Z$  and  $Y$  axes while transitions from the  $\Gamma_3$  level are dipole forbidden. To obtain the selection rules under an applied magnetic field, we treat the triplet levels as strictly degenerate and look for the linear combinations of the three unperturbed basis functions in (1b) which diagonalizes the linear Zeeman Hamiltonian, which in the case of quenched hole angular momentum is just  $H = 2\mu_B \mathbf{B} \cdot \mathbf{S}$ , where  $\mathbf{S}$  is the total spin angular momentum,  $\mathbf{S} = \mathbf{S}_h + \mathbf{S}_e$ . These combinations are easily calculated for an arbitrary  $\mathbf{B}$ -field direction and yield the standard energy eigenvalues,  $+\mu_B B \hbar$ , 0, and  $-\mu_B B \hbar$ . For an arbitrary  $\mathbf{B}$ -field direction, there are up to six inequivalent orientations of a  $C_{2v}$  defect, each with different admixtures of  $\Gamma_1$ ,  $\Gamma_3$ , and  $\Gamma_4$ . Computation of the polarization dependence of the Zeeman splittings of the  $P_0^0$  triplet ground state consists of evaluating the squared matrix elements,  $|\langle \Gamma_1 | e \mathcal{E} \cdot \mathbf{r} | \Psi_i \rangle|^2$ , where  $\Psi_i$  are the linear combinations of the states in (1b) which diagonalize the Zeeman Hamiltonian for a particular defect orientation. The results of this calculation are indicated in Fig. 2 by vertical bars under the experimental data. The simple theory predicts the qualitative behavior of the data, namely that the central component has a higher oscillator strength for transitions with the  $E$  vector perpendicular to the field than with it parallel, while the reverse obtains for the outer components. This behavior is the opposite of that expected for transitions from a pure spin triplet to a spin singlet in a system with full rotation symmetry. It is also at variance with the result obtained by assuming a  $p_Z$  hole state in the calculation.

### C. Valley-orbit effects

In previous stress measurements on the  $P_0^0$  line obtained under PL, we observed a definite nonlinearity in the shift rate of the  $\langle 001 \rangle$  data.<sup>14</sup> This was ascribed to the effects of valley-orbit mixing of the  $\Gamma_1$  electron state of the exciton with a higher-lying, at that point unidentified,  $\Gamma_3$  ( $T_d$ ) electron excited state. Based on the assumption of the free electron deformation potential,  $\Xi_u$ , and the use of unperturbed  $T_d$  electron states, we derived a valley-orbit splitting energy  $6\Delta_c$  of the order of 60 meV. In view of the stress data obtained in this study, we now propose that the  $P_3^0$  transition may be identified with the  $\Gamma_3$  ( $T_d$ ) excited state of the electron, and that the reduced valley-orbit energy which this implies is consistent with a reduced value of the deformation potential in the vicinity of the

defect.

For the moment we will assume that all the electron states have  $T_d$  symmetry. This is a reasonable approximation if the  $P_3^0$  line is due to a  $\Gamma_3$  electron, since such a state has a node in the central cell and would not feel the  $C_{2v}$  defect field too strongly. For the  $P_0^0$  and  $P_2^0$  states, which are assumed to be derived from  $\Gamma_1$  electron states, this approximation probably has less validity. The difference in the extent to which the  $\Gamma_1$  and  $\Gamma_3$  electron states sample the core immediately explains the presence of the large exchange energy splitting between the  $P_0^0$  triplet and the  $P_2^0$  singlet, and the apparent lack of any such splitting of the  $P_3^0$  level. If it is assumed that the no-phonon oscillator strength for these transitions derives largely from the high localization of the bound hole, then the increased strength of the  $P_3^0$  transition is just a reflection of the much higher degeneracy of this level due to the absence of an exchange splitting and the extra electron degeneracy.

The similarity of the splitting patterns of all three lines under  $\langle 111 \rangle$  stress (Fig. 4) agrees with the fact that such stress shifts all conduction-band valleys linearly by the same amount. The solid lines through the  $\langle 111 \rangle$  data in Fig. 4 have slopes given by a simultaneous least-squares fit to the  $P_0^0$  and  $P_2^0$  data, and are seen to give an adequate fit to the  $P_3^0$  data. Under  $\langle 001 \rangle$  stress, a stress-induced mixing should occur between the  $\Gamma_1$  and  $\Gamma_3$  levels.<sup>24</sup> This mixing introduces a nonlinearity into the  $\langle 001 \rangle$  shift rates which increases with decreasing valley-orbit interaction energy. This nicely accounts for the increase in curvature of the  $P_2^0$  shift rates relative to those of  $P_0^0$ . In our model the measured spectroscopic splitting between  $P_3^0$  and the other two lower energy transitions directly gives the valley-orbit splitting energy  $6\Delta_c$  of the electron bound in either the antisymmetric  $P_0^0$  ground state, or the symmetric  $P_2^0$  state. In this model the exchange interaction between the electron and the hole is just included into the central cell potential which scatters the electron into the various conduction-band valleys. The lines through the  $\langle 001 \rangle$  data in Fig. 4 represent fits to the data points based on the shift expressions of Wilson and Feher<sup>24</sup> for the valley-orbit states of electrons bound to substitutional donors in Si. The only free parameters in the fit are the orientational shift rates  $A_1$  and  $A_2$  from the preceding analysis, and the deformation potential for the conduction-band electrons. The parameters  $A_1$  and  $A_2$  largely model the orientational shift rates of the hole state, and this is assumed to be a constant for all three exciton transitions. The  $A_i$  values thus obtained are the experimental  $\langle 001 \rangle$  shift rates quoted in Table I. The values of  $6\Delta_c$  were derived from the spectroscopic splittings of the  $P_0^0$  and  $P_2^0$  states relative to the  $P_3^0$  transition, i.e., 36.3 and 24.9 meV, respectively, giving a mean value of 30.6 meV in the absence of the exchange interaction. In this simple model the two upper components of the  $P_3^0$  line which are observed under  $\langle 001 \rangle$  stress, are assumed to arise from the two different defect orientations of a rhombic I defect, labeled "a" and "b" in Fig. 4. The upward shift of these levels reflects the fact that they are derived solely from the four upward shifting conduction-band valleys. This model predicts two additional lines at lower energy, but only one is unambiguously identified.

The expected position of the extra line is indicated by the dotted line in Fig. 4. Like the upper  $P_3^0$  component, the lower one is so broad that it could easily contain a weak unresolved extra component. Cohen and Sturge<sup>2</sup> also reported considerable broadening of excitation lines of excited states of the  $NN_i$  pairs in GaP for  $i > 7$ . These excitation lines also overlapped the free-exciton continuum. The value of the electron deformation potential  $\Xi_u$  which produces the best fit is 6200 meV, which is considerably reduced from the value deduced from the far-infrared spectroscopy of shallow odd-parity donor levels, namely 8770 meV.<sup>25</sup> This value is consistent however with an observed reduction of  $\Xi_u$  for  $\Gamma_1$  states in the deeper substitutional donors in Si.<sup>25</sup> This suggests that the lattice is somewhat "stiffer" in its response to stress in the vicinity of the defect.

A  $\langle 110 \rangle$  stress is similarly expected to remove some of the electronic degeneracy of the  $P_3^0$  electron state. The lines through the  $P_3^0$  data in Fig. 4 represent the predictions of the above simple model in the case of  $\langle 110 \rangle$  stress, using the same deformation potential but using three different orientational shift parameters to model the linear shift rates. These are the experimental shift rates quoted in Table I. As in the case of the  $\langle 001 \rangle$  data, each of the three classes of orientationally distinct centers, labeled "c," "d," and "e," should show an additional two-fold splitting corresponding to the removal of some electronic degeneracy, but in practice only the lowest components are clearly seen. There is evidence of some additional splitting at higher energies but the inhomogeneous stress coupled with the intrinsic wide linewidths of the  $P_3^0$  components precludes positive identification.

It can be argued that the above description in terms of  $T_d$  symmetry is too simple and that at the very least one should attempt to include the effects of the local  $C_{2v}$  defect symmetry on the lowest-lying electron states. We have modeled the data assuming as an additional fitting parameter a constant internal strain field of the order of  $10^{-3}$ , in the spirit of Davies,<sup>22</sup> and more recently Thonke *et al.*<sup>9</sup> This procedure complicates the electron valley-orbit interaction matrix<sup>24</sup> somewhat, and does not offer a significantly better fit to these data.

#### IV. DISCUSSION

It is useful at this point to review what is now known about this particular isoelectronic defect. Substitutional In is known to introduce a very deep short-range potential for holes in Si. When the same sample-quenching procedure that is used to generate the 1118 meV In-related PL defect is applied to samples doped with the deeper acceptor Tl, a very similar set of lines is observed, having similar thermal, piezospectroscopic, and magnetic behavior but shifted downward in energy by an amount similar in magnitude to the difference in acceptor binding energies of the two deep acceptors.<sup>26</sup> Thus it is clear that the central cell potential of the acceptor is important in the binding of these excitons. Presumably the excess charge of the acceptor is neutralized by a nearby constituent, e.g., an interstitial donor, rendering the whole defect electrically neutral. In the simple binding scheme of Hopfield *et al.*<sup>1</sup> one might expect to see an effective masslike

excited-state spectrum of a more loosely bound electron, but this is certainly not observed in this case. The average value of  $6\Delta_c = 30.6$  meV obtained for the valley-orbit energy of the electron should be compared to values of 13.01, 22.5, and 37.11 meV for P, As, and Bi donors, respectively.<sup>27</sup> Thus the short-range attractive potential for the electron is relatively deep by comparison with the simple substitutional donors in Si. The designation of  $P_3^0$  as due to an excited valley-orbit state of the electron places the donor ionization limit very close to 31 meV above the  $P_3^0$  energy according to effective-mass theory, which is expected to give useful predictions for the higher-lying electron states. This is well above the non-phonon free-exciton edge and accounts for the observation that the thermal dissociation energy of the exciton is identical to the spectroscopic localization energy with respect to the free-exciton energy.<sup>28</sup> This is different from the usual case of isoelectronic centers as described by Hopfield *et al.*<sup>1</sup> in which the first bound particle has a bound state even in the absence of the second particle. In such centers, e.g., the  $NN_i$  pairs in GaP with  $i < 8$ , the binding energy of the first bound particle is given by the difference between the total binding energy of the exciton ground state, and the binding energy of the weakly bound particle as determined from the series limit of its excited states.<sup>2</sup> For the case of the In isoelectronic center this binding energy would be negative, so it appears that the central cell potential of the In-related isoelectronic binding center is not strong enough to bind a hole alone, and the model of Hopfield *et al.*<sup>1</sup> is clearly not applicable. Similar effects are observed by Cohen and Sturge<sup>2</sup> for the  $NN_i$  pairs with  $i > 7$ .

The clear absence of a bound state for the isolated hole together with the evidence that both particles feel an attractive central cell potential can be explained by an additional binding mechanism such as Allen's strain-field model.<sup>3</sup> Monemar *et al.*<sup>4</sup> and Gislason *et al.*<sup>5</sup> have invoked a strain mechanism to account for the extremely large localization of both particles which they observe in excitons bound to Cu-related isoelectronic defects in GaP. A strain field can be attractive to both particles and could provide the extra binding energy which the above data require. Such a field could arise from the internal hydrostatic and shear components of the relatively large defect components. In addition, lattice relaxation after exciton capture could enhance the effect of such a strain well. The strong phonon sidebands observed in PL are indicative of substantial lattice relaxation. It is important to note however that a strain field is typically long-ranged, with a  $1/r^3$  dependence, and it is not clear whether such a field could cause the large valley-orbit splitting indicated by the above data.

The question as to the precise constituents of this defect must still remain open. The role of substitutional In in the defect has been confirmed by a previous study.<sup>26</sup> The defect symmetry has been unambiguously determined here to be  $C_{2v}$ . The simplest candidate for the extra constituent would be the presence of an interstitial donor in the nearest  $T_d$  interstitial site. This constituent must be quite mobile given the stress-induced reorientation observed in PL at 4.2 K.<sup>14</sup>

In summary, we have used uniaxial stress and magnetic field perturbations to explain the excited-state spectrum of the 1118 meV In-related isoelectronic bound exciton. A specific model for the electron- and hole-state symmetries was confirmed by polarization measurements obtained under a magnetic field. The exciton ground state was shown to be split into a triplet and singlet with a relatively large exchange interaction energy, confirming a high degree of localization of both particles. A higher-lying excited state was shown to correspond to a valley-orbit excited state of the bound electron. The usual isoelectronic binding mechanism of Hopfield, Thomas, and Lynch<sup>1</sup> was shown to be inappropriate for this defect, as has been found to be the case for a variety of recently discovered

centers in GaP.<sup>4,5</sup> As in those cases, the internal strain field of the defect is most likely responsible for the enhanced binding of both particles.

#### ACKNOWLEDGMENTS

The authors are grateful to Dr. G. Kirczenow for useful discussions regarding the symmetries of the bound exciton states. The research was supported by Natural Sciences and Engineering Research Council (NSERC) Grant No. U0069. S.P.W. received additional support from NSERC and from Simon Fraser University. M.L.W.T. gratefully acknowledges support from the Alfred P. Sloan Foundation.

- <sup>1</sup>J. J. Hopfield, D. G. Thomas, and R. T. Lynch, *Phys. Rev. Lett.* **17**, 312 (1966).
- <sup>2</sup>E. Cohen and M. D. Sturge, *Phys. Rev. B* **15**, 1039 (1977).
- <sup>3</sup>J. W. Allen, *J. Phys. C* **4**, 1936 (1971).
- <sup>4</sup>B. Monemar, H. P. Gislason, P. J. Dean, and D. C. Herbert, *Phys. Rev. B* **25**, 7719 (1982).
- <sup>5</sup>H. P. Gislason, B. Monemar, P. J. Dean, and D. C. Herbert, *Phys. Rev. B* **26**, 827 (1982).
- <sup>6</sup>J. Wagner and R. Sauer, *Phys. Rev. B* **26**, 3502 (1982).
- <sup>7</sup>M. L. W. Thewalt, S. P. Watkins, U. O. Ziemelis, E. C. Lightowers, and M. O. Henry, *Solid State Commun.* **44**, 573 (1982).
- <sup>8</sup>D. Labrie, T. Timusk, and M. L. W. Thewalt, *Phys. Rev. Lett.* **52**, 81 (1983).
- <sup>9</sup>K. Thonke, A. Hangleiter, J. Wagner, and R. Sauer, *J. Phys. C* **18**, L795 (1985).
- <sup>10</sup>J. Wagner, A. Dornen, and R. Sauer, *Phys. Rev. B* **31**, 5561 (1981).
- <sup>11</sup>G. S. Mitchard, S. A. Lyon, K. R. Elliott, and T. C. McGill, *Solid State Commun.* **29**, 425 (1979). These authors proposed an isoelectronic origin for this family of lines, but their original explanation attributed the lines to three different binding centers, whereas it was subsequently shown that only one center was responsible. See Ref. 13 for relevant references.
- <sup>12</sup>For a review see Refs. 13 and 14.
- <sup>13</sup>S. P. Watkins, M. L. W. Thewalt, and T. Steiner, *Phys. Rev. B* **29**, 5727 (1984).
- <sup>14</sup>S. P. Watkins and M. L. W. Thewalt, *Can. J. Phys.* **63**, 1074 (1985).
- <sup>15</sup>J. Wagner and R. Sauer, *Phys. Rev. B* **27**, 6568 (1983).
- <sup>16</sup>R. W. Wallace, *IEEE J. Quantum Electron.* **QE-8**, 819 (1972).
- <sup>17</sup>I. Shoshan, N. Danon, and U. Oppenheim, *J. Appl. Phys.* **48**, 4495 (1977).
- <sup>18</sup>A. A. Kaplyanski, *Opt. Spectrosc. (USSR)* **16**, 329 (1964).
- <sup>19</sup>P. Clifton, G. Davies, and E. C. Lightowers, *J. Phys. C* **17**, L889 (1984).
- <sup>20</sup>P. J. Dean, R. A. Faulkner, and E. G. Shonherr, in *Proceedings of the 10th International Conference on the Physics of Semiconductors*, edited by S. P. Keller, J. C. Hensel, and F. Stern (U.S. Atomic Energy Commission, Springfield, Virginia, 1970), p. 286.
- <sup>21</sup>J. W. Morgan and T. N. Morgan, *Phys. Rev. B* **1**, 739 (1970).
- <sup>22</sup>G. Davies, *J. Phys. C* **17**, 6331 (1984).
- <sup>23</sup>G. F. Koster, J. O. Dimmock, R. G. Wheeler, and H. Statz, *Properties of the Thirty-Two Point Groups* (M.I.T. Press, Cambridge, Massachusetts, 1963).
- <sup>24</sup>D. K. Wilson and G. Feher, *Phys. Rev.* **124**, 1068 (1961).
- <sup>25</sup>V. J. Tekippe, H. R. Chandrasekhar, P. Fisher, and A. K. Ramdas, *Phys. Rev. B* **6**, 2348 (1972).
- <sup>26</sup>M. L. W. Thewalt, U. O. Ziemelis, R. R. Parsons, *Phys. Rev. B* **24**, 3655 (1981).
- <sup>27</sup>A. K. Ramdas and S. Rodriguez, *Rep. Prog. Phys.* **44**, 1298 (1981).
- <sup>28</sup>M. L. W. Thewalt, U. O. Ziemelis, S. P. Watkins, and R. R. Parsons, *Can. J. Phys.* **60**, 1691 (1982).